
Characterizing the spread of CoViD-19

Dean Karlen^{1,2}

July 13, 2020

Abstract

Since the beginning of the epidemic, daily reports of CoViD-19 cases, hospitalizations, and deaths from around the world have been publicly available. This paper describes methods to characterize broad features of the spread of the disease, with relatively long periods of constant transmission rates, using a new population modeling framework based on discrete-time difference equations. Comparative parameters are chosen for their weak dependence on model assumptions. Approaches for their point and interval estimation, accounting for additional sources of variance in the case data, are presented. These methods provide a basis to quantitatively assess the impact of changes to social distancing policies using publicly available data. As examples, data from Ontario and German states are analyzed using this framework. German case data show a small increase in transmission rates following the relaxation of lock-down rules on May 6, 2020. By combining case and death data from Germany, the mean and standard deviation of the time from infection to death are estimated.

Keywords

CoViD-19, Epidemiology, Public case data, Epidemic growth, discrete time

1 Introduction

The CoViD-19 epidemic gained world-wide attention in March 2020 as the number of cases began to rise rapidly. For most people, this was their first experience with an epidemic and public health measures enacted to reduce social contact. While these measures caused major disruptions in daily life, they eventually reduced the rate of growth in case numbers. Several regions saw localized outbreaks, particularly in long term care facilities and meat processing facilities. After a few months, social distancing regulations began to be relaxed, with the intention that viral spread would kept at a manageable level.

While this describes the general experience in many western nations, there are significant differences seen within some nations, in their timelines and growth rates. This paper presents methods to characterize differences in the spread of CoViD-19 that can be deduced from publicly available data. This information can be useful for assessing the current situation and to identify successful strategies to reduce transmission.

This paper introduces a new general-purpose modelling framework developed to study the spread of CoViD-19. A simple model, chosen to interpret CoViD-19 daily data, is described and its properties are investigated. Comparative statistics, chosen to have weak dependence on model assumptions, are defined. Data analysis approaches to estimate model parameters and their uncertainties are described, along with studies of simulated data.

¹University of Victoria

²TRIUMF

Corresponding author:

Dean Karlen, Department of Physics and Astronomy, University of Victoria, Victoria, BC, Canada, V8W 2Y2.

Email: karlen@uvic.ca

2 Modeling framework

The python Population Modeller (pyPM¹), is a general framework for building models of viral spread using discrete-time difference equations. A pyPM model is an object that consists of a set of population objects connected by an ordered list of directional connector objects. Parameter objects are used to manage the various adjustable parameters necessary to define a specific model. The object oriented design separates the task of model design from numerical implementation which reduces the risk of implementation errors and simplifies the process of model redesign. The model object, containing the model design and its parameters, can be saved in small files, allowing for a multitude of models to be cataloged.

Two main reasons favor the use of discrete-time difference equations for this study, over the traditional ordinary differential equation approach. Firstly, with discrete-time difference equations, it is straightforward to implement arbitrary time delay distributions, such as normal distributions with mean and standard deviations specified as parameters. Secondly, the purpose of the modeller is to interpret publicly available data reported as daily counts, and with a step size of one day, daily expectations or simulated daily counts are computed directly. The daily values are saved as a time series in the population objects, and referred to as “histories”.

The basic connector, called a propagator, transfers a fraction of incoming members from one population (referred to as the “from-population”) to another (referred to as the “to-population”) according to a delay distribution. The delayed transfer is accomplished by having each population maintain a list of incoming contributions for each day in the future. A “splitter” connector divides the incoming “from-population” members to two or more “to-populations”. A “multiplier” connector produces a number of new members in the “to-population”, based on the sizes of the “from-populations” and forms the basis of the infection cycle. “Subtractor” and “Adder” connectors subtract from or add to populations without delay.

Prior to taking a time step, the connectors are processed in order, with each calculating the future contributions to its “to-populations”, given the number of “from-population” members arriving at the next time step. After all calculations are completed, the time step is taken, by having each population extend its history with a new value, consisting of the previous day’s number and the future contribution for that day.

As an illustration, consider a model in which a fraction f_u of the symptomatic population S are admitted into ICU, population U , and those are split into two populations, a fraction f_v are treated with a ventilator V , and the remaining are released without ventilation, W . If the current time step is t , the expected incoming population for S is $E[\Delta S_{t+1}]$. Future expected contributions to population U arising from that incoming population to S are:

$$\begin{aligned}
 E[\Delta U_{t+1+j}] &= f_u E[\Delta S_{t+1}] \beta_{uj} \\
 \beta_{u0} &= \int_{-\infty}^{\frac{1}{2}} g_u(t) dt \\
 \beta_{uj} &= \int_{j-\frac{1}{2}}^{j+\frac{1}{2}} g_u(t) dt \quad \text{for } j > 0
 \end{aligned}$$

where g_u is the distribution that defines the delay in the symptomatic population transferring to the ICU population. Following that calculation, the future contributions to the ventilated and non-ventilated populations, V and N , are calculated in a similar fashion,

$$\begin{aligned}
 E[\Delta V_{t+1+j}] &= f_v E[\Delta U_{t+1}] \beta_{vj} \\
 E[\Delta W_{t+1+j}] &= (1 - f_v) E[\Delta U_{t+1}] \beta_{nj}
 \end{aligned}$$

Alternatively, instead of calculating expectation values, the calculations can be performed as a stochastic simulation, where population sizes are defined by integers, for example,

$$b = B(\Delta S_{t+1}, f_u)$$

$$\Delta U_{t+1+j} = M(b, \beta_{uj})$$

where B returns a binomial variate and M returns multinomial variates. The stochastic simulation of the infection cycle would use a Poisson variate if infections were described by independent events. To account for grouping of infections, negative binomial variates are used, parameterized by the mean μ and $p_{nb} \in (0, 1)$, such that the variance is μ/p_{nb} . The stochastic calculations are useful for checking for bias and for evaluating standard deviations of estimators.

3 Model for characterizing the spread of CoViD-19

The pyPM reference model 2.3 is a simple model developed to characterize the spread of CoViD-19. It includes an infection cycle connected to populations that correspond to publicly available data for cases, deaths, and hospitalization, including ICU and ventilator use.

3.1 Infection cycle model

Results in this paper use pyPM reference model 2.3 as the nominal model, and its infection cycle is defined by three connectors. Firstly, for each day, the expected number of new infections is calculated as:

$$E[\Delta I_{t+1}] = \alpha \frac{E[S_t]}{E[N_t]} E[C_t]$$

where α is the transmission rate, S the susceptible population, N the total population, and C the circulating contagious population. In the initial stages of an epidemic, when almost the entire population is susceptible, α represents the average number of people that a contagious person infects in one day. Its value can be considered to be linearly proportional to the number of contacts and closeness of contact between individuals, and therefore it is a parameter that is linearly proportional to social distancing measures.

The second connector propagates a fraction of the newly infected population to the circulating contagious population, with a delay distribution modeling the so-called “latent period”. The third connector reduces the size of the circulating contagious population using a propagator to a removed population and a subtractor is used to remove them. The propagator uses a delay distribution to represent the “contagious circulation period” which arises from all ways that contagious individuals become unable to infect others, including quarantine, hospitalization, natural recovery, or death.

In the initial stages and when the transmission rate and circulation time are constant, the “steady state” solution to the time difference equations has the expected contagious population being exponential in time,

$$E[C_{t+1}] = (1 + \delta)E[C_t].$$

The parameter describing fractional daily growth, identified as δ in this paper, is often referred to as r in epidemiology literature. To ensure that the initial state corresponds to a “steady state” solution, the model uses a “boot-strap” approach. A state with a very small expectation value for the contagious population size is allowed to grow until the target contagious population for the initial state is reached. While only the initial contagious population needs to

be specified, all other populations will be assigned non-zero expectation values at the initial state that correspond to a “steady state” solution.

The infection cycle model is purposefully simplistic, being described by a homogeneous population. This reduces the number of parameters and characterizes the epidemic spread for those groups in the population that contribute the greatest numbers to cases, hospitalization, or deaths. While the pyPM framework includes ensembles for modelling heterogeneous populations, there is little public data available to constrain the many additional parameters. For this paper, we characterize the spread using a homogeneous model.

3.2 Modeling case reporting, hospitalization, and deaths

The pyPM reference model 2.3 connects the contagious population to the symptomatic population and from symptomatic to reported (positive test cases), icu admission, and non-icu admission populations. It also has an independent propagator from contagious to recovery or death. Each of these connectors is parametrized by a fraction and a normal delay distribution.

If testing captures a constant fraction of contagious individuals, then the expected cases will follow the contagious population trajectory with a time lag. The case data can therefore be used to estimate δ during these periods without reference to a particular model. Hospitalization and death rates provide additional measures of the infection trajectory. When these are seen to follow different growth curves, this may indicate differences in transmission by age or other factors, since these data are unequal samplings of the infected population.

3.3 Model dependence on transmission rate estimators

It would be useful to characterize the phases of an epidemic with a transmission rate parameter like α that in some sense is linearly proportional to social distancing. By doing so, statements can be made about relative levels of social distancing observed in past phases and levels required going forward. Unfortunately, unlike for δ , estimating the transmission rate, α , from case data sensitively depends on the latent and circulation delay distributions which are not well known. The well known parameter to characterize the growth rate, the reproduction number R_0 , also suffers from strong model dependence^{2,3}.

Figure 1 shows how changing the delay distributions affects the relation between the exponential growth and the transmission rate. Increasing the mean circulation period increases δ , since contagious individuals have more time to infect more people. Increasing the latent period reduces δ for a growth phase and increases δ for a decline phase, since newly infected individuals take longer to become contagious thereby reducing the feedback responsible for producing the exponential growth or decline.

To further illustrate the sensitivity to the delay distribution parameters, consider the default conditions for pyPM reference model 2.3, which describes a period of growth followed by a period of decline:

- C_0 (initial contagious population): `cont_0 = 10`
- α_0 (initial transmission rate): `alpha_0 = 0.4`
- t_1 (day # for transmission rate change): `trans_rate_1_time = 20`
- α_1 (new transmission rate): `alpha_0 = 0.1`
- ℓ_μ (latent period mean): `cont_delay_mean = 5 (days)`
- ℓ_σ (latent period standard deviation): `cont_delay_sigma = 3 (days)`
- c_μ (circulation period mean): `removed_delay_mean = 7 (days)`
- c_σ (circulation period standard deviation): `removed_delay_sigma = 3 (days)`

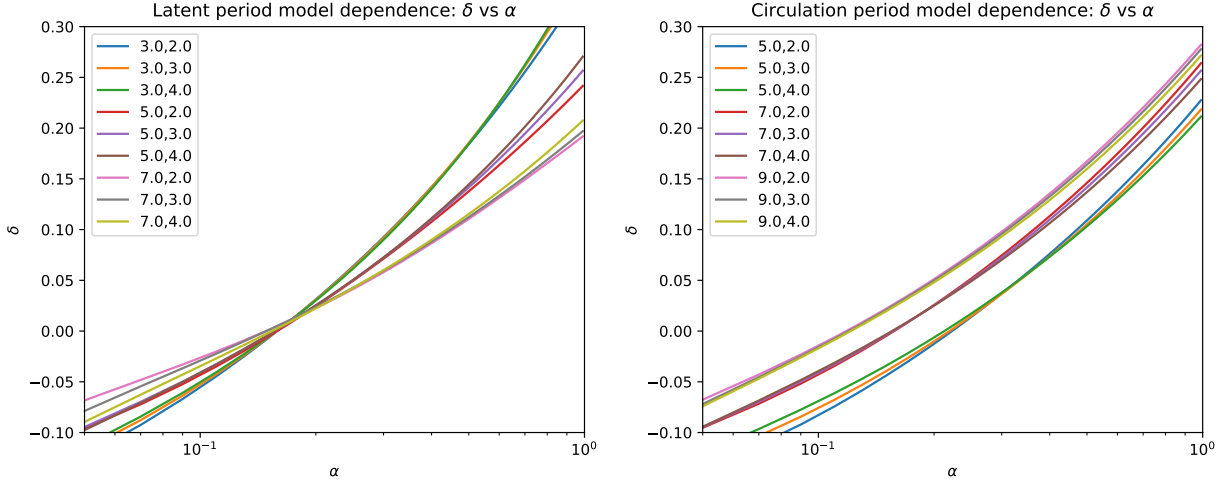


Figure 1. The relation between the exponential growth rate parameter δ and the transmission rate parameter α is shown for several choices for the latent period parameters (left) and circulation period parameters (right). The legend shows the means and standard deviations for the latent (left) and circulation (right) normal delay distributions (in days). The nominal model has $\ell_\mu = 5$, $\ell_\sigma = 3$, $c_\mu = 7$, $c_\sigma = 3$.

If case data produced according to this nominal model, is analyzed with a modified model, having different assumptions for the latent and circulation periods, the estimators for α_0 and α_1 will be biased. To estimate the bias, assume that estimators for the model independent parameters, δ_0 and δ_1 , are unbiased. Given a choice for the delay parameters, the relation between $\hat{\alpha}$ and $\hat{\delta}$ can be found empirically

$$\hat{\alpha} = \hat{\alpha}(\hat{\delta} \mid \ell_\mu, \ell_\sigma, c_\mu, c_\sigma),$$

which would be the inverse of the functions shown in Fig. 1. With sufficient statistics, the bias in the transmission rate estimators would be approximately

$$b = E[\hat{\alpha}] - \alpha = \hat{\alpha}(E[\hat{\delta}] \mid \ell_\mu, \ell_\sigma, c_\mu, c_\sigma) - \alpha.$$

Table 1 shows the expectation values and the relative bias for the transmission rate estimators for reasonable alternative delay parameter values. For many cases, the bias is larger than typical standard deviations of the estimators (statistical uncertainty). When alternative latent period parameters are used, the bias for the growth and decline estimators have opposite sign.

From this study, we find that transmission rates, or relative transmission rates, are not good choices for characterizing growth or decline due to their sensitivity to poorly known model parameters. Instead, in this paper we use the nominal model parameters to form estimators for α and convert those to estimators for δ . As shown in section 4, the biases in estimators for δ are found to be small.

Table 1. The size of transmission rate estimator biases for alternative delay parameter values for an epidemic having a growth period followed by decline, as described in the text. The last column shows that the ratio of the estimated transmission rates varies from 3 to 6 depending on the delay parameters.

ℓ_μ	ℓ_σ	c_μ	c_σ	$E[\hat{\alpha}_0]$	$\frac{b_0}{\alpha_0}$ (%)	$E[\hat{\alpha}_1]$	$\frac{b_1}{\alpha_1}$ (%)	$E[\hat{\alpha}_0]/E[\hat{\alpha}_1]$
3	2	7	3	0.333	-17	0.114	14	2.9
3	3	7	3	0.334	-16	0.112	12	3.0
3	4	7	3	0.338	-15	0.110	10	3.1
5	2	7	3	0.407	2	0.103	3	4.0
5	3	7	3	0.400	0	0.100	0	4.0
5	4	7	3	0.396	-1	0.100	0	4.0
7	2	7	3	0.497	24	0.079	-21	6.3
7	3	7	3	0.489	22	0.085	-15	5.8
7	4	7	3	0.477	19	0.092	-8	5.2
5	3	5	2	0.503	26	0.154	54	3.3
5	3	5	3	0.516	29	0.148	48	3.5
5	3	5	4	0.524	31	0.139	39	3.8
5	3	7	2	0.390	-2	0.102	2	3.8
5	3	7	3	0.400	0	0.100	0	4.0
5	3	7	4	0.411	3	0.098	-2	4.2
5	3	9	2	0.330	-18	0.072	-28	4.6
5	3	9	3	0.336	-16	0.074	-26	4.5
5	3	9	4	0.344	-14	0.075	-25	4.6

3.4 Model dependence on contagious population estimators

In addition to the rate of growth or decline, represented by δ , the size of the circulating contagious population is important to characterize the state of the epidemic. This is not directly measured by case data and estimators are affected by many unknown factors, such as the fraction of infected individuals who are tested. While the absolute number may be poorly known, a relative indicator that has weaker model dependence would be useful to indicate relative prevalence between two regions or between two different periods within a region. For this purpose, case data is analyzed using the nominal model, and the deduced contagious population is scaled by the ratio of total cases to total infections. The result, UC , for “uncorrected circulating contagious population”, would need to be divided by the fraction of infected individuals tested, to be an estimate for the absolute size of the contagious population. The correction factor is not necessary to compare the relative prevalence in regions with similar testing policy.

Just as for α , the estimator for UC depends on the latent and circulation delay parameters. To illustrate the sensitivity, the same combinations for delay parameters are considered and the ratio of $UC_{\text{mod}}/UC_{\text{nom}}$ is shown in Fig. 2 for the same conditions as described in section 3.3. Large deviations up to about 30% are seen, but this effect is small compared to the observed range of prevalence which spans several orders of magnitude.

3.5 Modeling localized infection outbreaks

If a large localized infection outbreak occurs during a period where social distancing policy is being followed consistently, the indicators for nominal infection growth/decline should be unaffected. The rapid growth in count rates is not a result of changing social behaviour that would lead to a new infection trajectory. Instead, once the outbreak runs its course, the region would continue with the same growth/decline as before the outbreak.

To model this situation, a burst of infections is injected into the infected population, with the number and date of burst optimized to match the case data. During a period of increasing social distancing, a rapid rise in cases would be a clear signal for an infection outbreak. During a period when social distancing rules are being relaxed, an increase in cases could be a result of the expected increase in transmission or due to a new outbreak. In absence of other

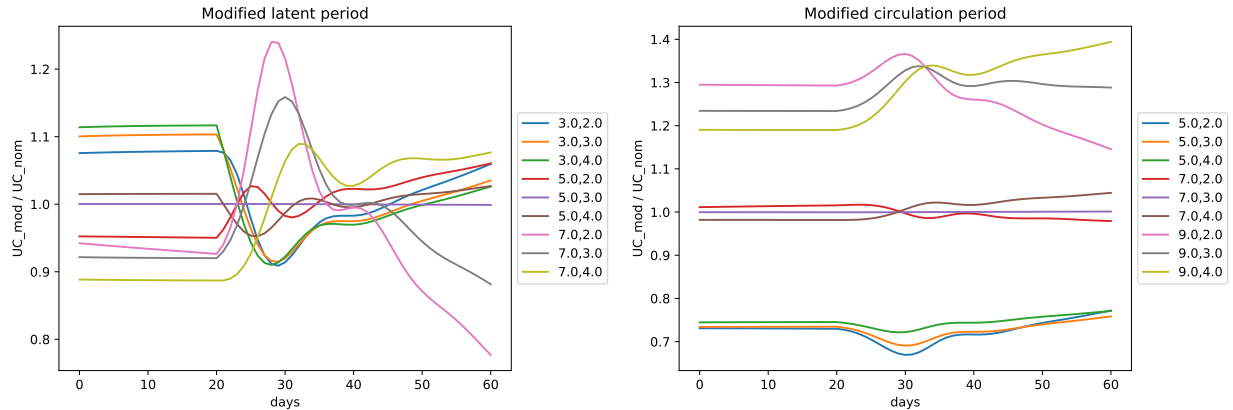


Figure 2. The expectation of the estimator for “uncorrected circulating contagious population” using a modified model compared to that using the nominal model. The adjusted latent period and circulation delay parameters (μ and σ) are shown in the legend.

information that can distinguish these two hypotheses, it may be necessary to wait until for the case data itself to identify whether or not the region is experiencing a new rate of growth.

3.6 Modeling case reporting

The daily number of new cases in a region is the publicly available indicator with the largest statistics and smallest time lag. The pyPM reference model 2.3 models case reporting by propagating a fraction ($f_s = 0.9$) of the newly contagious population to the symptomatic population and a fraction ($f_r = 0.8$) of those to the reported population. The propagation time delays are described by normal distributions ($\mu_s = 2$, $\sigma_s = 1$ days) and ($\mu_r = 3$, $\sigma_r = 1$ days) respectively. The size of the reported population is compared directly with publicly available case data to characterize the spread of CoViD-19. The uncertainties in the fractions contribute to systematic uncertainty in estimating the size of the contagious populations, and the uncertainties in the delay parameters contribute to uncertainty in identifying transition dates from the case data.

During the initial phase of the epidemic in western nations, in March 2020, testing policy and availability were changing significantly. This may account for the fact that in many regions, including in Canada and the United States, the number of cases did not follow an exponential growth trajectory in early March. After that, the growth in number of cases are generally well described by models with relatively long periods of constant transmission and testing rates, even though testing availability generally increased. This suggests that revised testing policies enacted after March did not substantially change the fraction of infected individuals getting tested. Should a testing or reporting policy change cause a rapid rise in cases, this could be misinterpreted as a reporting anomaly or a localized outbreak, but this will not cause δ to be overestimated. It is the exponential growth of cases that determines δ , not the absolute number of cases.

Estimating the growth and size of the contagious population from case data, and interval estimation in particular, presents a challenge due to the large variance in the daily reported numbers. Occasionally, a very large number of cases is reported on one day, as a backlog of cases clears some bottleneck in the reporting process. These anomalies are normally announced and they are modelled by an injection into the reported population. Even ignoring those rare situations, daily case numbers have variance that far exceeds that expected in a model with independent infected individuals being tested as they become symptomatic. The pyPM model includes variation that arises from the reporting process itself, in which a variable fraction of cases are held back and reported the next day. The fraction is drawn from a uniform distribution between rn and 1, where rn is the reporting noise parameter. This produces a

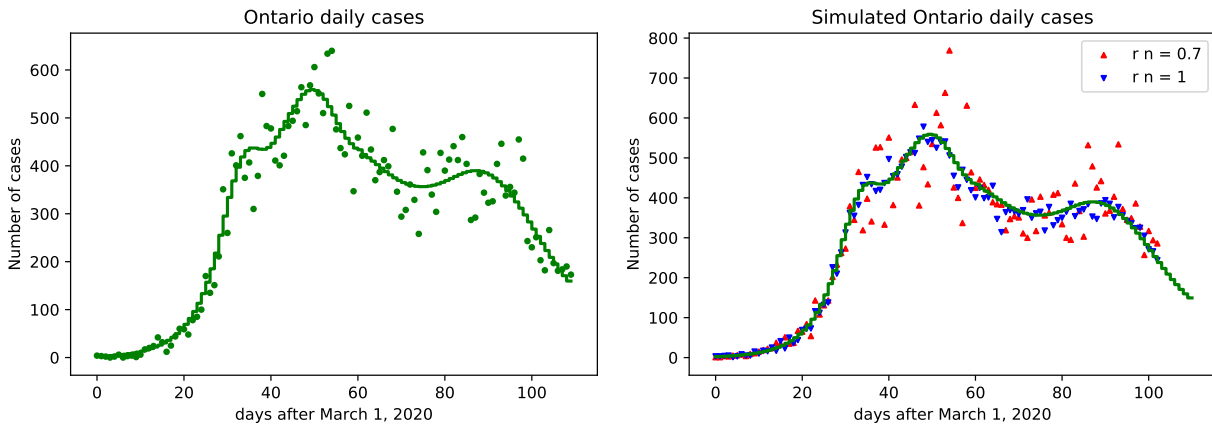


Figure 3. Left: Points show the daily cases reported from the province of Ontario and the curve shows the expectations for each day from the model. Right: Simulations with no reporting noise ($r_n=1$) and with reporting noise ($r_n=0.7$) tuned to match the data goodness of fit statistic. The simulations use the negative binomial parameter for the infection cycle $p_{nb}=0.1$. To help the visual comparison, simulations were chosen that have total infections close to the expected value.

negative autocorrelation between one day and the next, which can be compared with actual data. A second parameter, noise backlog, is provided to allow that only a fraction of the backlog being reported the next day, to reduce the autocorrelation effect in the data. By including this additional source of variance, the intervals for the growth parameter estimates can grow by a factor of 2 or more.

As an example, the daily cases from the province of Ontario is shown, along with the expectations from the model fit to that data in Fig. 3. The first 110 days are generally described by two transitions of transmission rate (on day 26 and 44) and one broad reporting anomaly centered at day 91. The day-to-day variation is larger than the model with no reporting noise. In many jurisdictions, the effect of reporting noise is even larger than this. To match the goodness of fit, calculated by assuming the daily data follow a Poisson distribution, the reporting noise parameter is set to 0.7. Other provincial and state data typically require additional reporting noise with this parameter set between 0 and 0.5. To match the goodness of fit for the cumulative cases, the negative binomial parameter for the infection cycle p_{nb} is set to 0.1. These parameters were set by looking at the goodness of fit for 10 fitted simulation samples.

3.7 Modeling hospitalization and death reporting

The pyPM reference model 2.3 models hospitalization data by propagating a fraction of the newly symptomatic population to icu and non-icu hospitalized populations, and a fraction of the icu admissions are propagated to the ventilated population. Each of these use by normal time delay distributions. Deaths are modelled by propagating a fraction of the newly contagious population with a normal time delay distribution.

4 Point estimates using case data

As indicated in section 3.6, the variance in the daily case counts exceeds that expected in a simple model, and therefore an additional source of variation is included in the model to represent variation in daily reporting. A more significant complication is that the daily cases do not represent outcomes of independent random variables. Having a larger than expected number of infections for one day will generally result in larger than expected number of cases (and a larger than expected number of infections) in subsequent days. This effect is illustrated in Fig. 4.

The standard approach of maximum likelihood estimation is difficult to apply given the challenges in defining an appropriate likelihood function. Instead, point estimates for model parameters are the combination that best reproduces

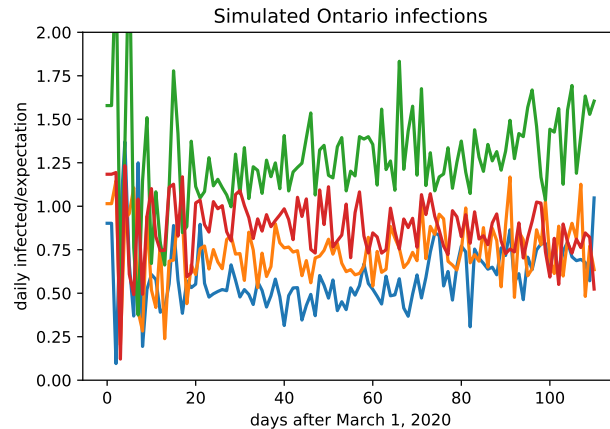


Figure 4. The ratio of daily new infections to expected new infections are shown for four simulations of the Ontario model to illustrate that daily new cases are not outcomes of independent random variables. The simulations use the negative binomial parameter for the infection cycle $p_{nb}=0.1$.

Table 2. Descriptive statistics for point estimates for the 1000 simulated samples using the Ontario model. The column labeled σ_{stat} shows the standard deviation of the point estimates.

parameter	truth	mean	σ_{stat}	bias (in σ_{stat})
cont_0	29.0	26.4	6.3	-0.41
alpha_0	0.632	0.638	0.033	0.19
alpha_1	0.202	0.205	0.007	0.42
alpha_2	0.128	0.127	0.004	-0.03
anomaly_1_n	3727	3722	598	-0.01

the cumulative case history by minimizing the sum of the squares of the differences between the model expectations and data. The following model parameters are estimated:

- initial size of contagious population
- transmission rates for each period (and end dates)
- sizes of infection outbreaks (and dates)
- size of reporting anomalies (and dates)

Biases and standard deviations of the estimators are found by fitting simulated samples. As an example, the distributions of point estimates for 1000 simulated samples using the Ontario model are found to each be approximately normal and only the final two (α_2 and number in reporting anomaly) have strong correlation ($\rho \approx -0.6$). The standard deviations of the transmission rate estimators are found to be approximately 5% of the true values. Table 2 shows that the biases are less than 1 standard deviation for all parameters.

As discussed in section 3.3, characterizing the growth in terms of δ instead of α has the benefit of being less model dependent. This is illustrated in table 3 which shows the point estimates for α and δ for different choices for the parameters that define the latent and circulation periods in the infection cycle. For this distribution of delay parameters, the standard deviation of the α parameter estimates, indicated in the table as σ_{sys} , are significantly larger than standard deviations in the estimators, σ_{stat} . For δ , the systematic and statistical standard deviations are nearly the same. The systematic uncertainty is characterized by σ_{sys} , provided the range of variation of the delay parameters corresponds to about 1 standard deviation in the prior beliefs for these quantities. The range of the delay parameters were chosen using the summary provided by the Public Health Agency of Canada Modelling Group⁴.

Table 3. Estimates for growth parameters for Ontario data from March 1 - June 17 under different latent and circulation period parameters. For these fits, the transmission rate transition dates and the outbreak date were fixed. Systematic uncertainty is characterized by the standard deviation of the parameter estimates for the distribution of delay period parameters and statistical uncertainties are taken from Table 2.

ℓ_μ	ℓ_σ	c_μ	c_σ	$\hat{\alpha}_0$	$\hat{\alpha}_1$	$\hat{\alpha}_2$	$\hat{\delta}_0$	$\hat{\delta}_1$	$\hat{\delta}_2$
3	2	7	3	0.514	0.197	0.135	0.188	0.029	-0.020
3	3	7	3	0.520	0.199	0.135	0.192	0.030	-0.020
3	4	7	3	0.531	0.200	0.134	0.195	0.030	-0.019
5	2	7	3	0.634	0.201	0.128	0.171	0.025	-0.021
5	3	7	3	0.632	0.202	0.128	0.177	0.027	-0.019
5	4	7	3	0.635	0.203	0.127	0.182	0.027	-0.020
7	2	7	3	0.754	0.202	0.119	0.155	0.026	-0.010
7	3	7	3	0.755	0.203	0.119	0.160	0.027	-0.014
7	4	7	3	0.754	0.204	0.118	0.167	0.025	-0.021
5	3	5	2	0.740	0.268	0.181	0.172	0.022	-0.024
5	3	5	3	0.778	0.270	0.179	0.174	0.024	-0.022
5	3	5	4	0.811	0.269	0.173	0.175	0.026	-0.021
5	3	7	2	0.608	0.199	0.128	0.176	0.025	-0.020
5	3	7	3	0.632	0.202	0.128	0.177	0.027	-0.019
5	3	7	4	0.662	0.205	0.126	0.178	0.028	-0.019
5	3	9	2	0.545	0.161	0.099	0.179	0.030	-0.015
5	3	9	3	0.567	0.163	0.099	0.182	0.029	-0.016
5	3	9	4	0.583	0.167	0.098	0.181	0.030	-0.019
mean				0.648	0.206	0.131	0.177	0.027	-0.019
σ_{sys}				0.096	0.032	0.025	0.010	0.002	0.003
σ_{stat}				0.033	0.007	0.004	0.008	0.004	0.003
$\sigma_{\text{sys}}/\sigma_{\text{stat}}$				3.0	4.9	6.3	1.2	0.7	1.2

4.1 Using hospitalization data to characterize growth

Public data from regions with significant CoViD-19 hospitalizations can be used as an alternative measure of the exponential growth rate parameter δ . In the simplified homogeneous model assumed for this paper, daily hospital admissions and the number of individuals in hospital will also follow exponential growth or decline during periods of constant transmission rate. For the Ontario public hospitalization data corresponding to the case data used for the fits in Table 3, there is sufficient data to estimate δ_2 . The results are found to be $\hat{\delta}_{2h} = -0.003 \pm 0.012$ (in-hospital data) and $\hat{\delta}_{2i} = -0.022 \pm 0.010$ (in-ICU data), both consistent with the case data estimate ($\hat{\delta}_2 = -0.019 \pm 0.003$), albeit with much larger statistical uncertainties, given the limited number of hospitalizations as compared to positive tests.

Differences between case data and hospitalization estimates for δ could arise in models with heterogeneous populations, accounting for the fact that the population requiring hospitalization for CoViD-19 is older than the population tested positive for the disease, and the transmission rates and circulation periods may differ by age. In British Columbia, for example, the median age for the hospitalized population is 69 years, compared to 51 years for the population who have tested positive⁵.

5 Analyses of German state data

Data from German states represent samples from populations subject to the same public health measures and testing policies. Germany enacted strict lock-down measures on March 22, 2020 as cases were rising rapidly. Following the decline in cases in April, the measures were relaxed on May 6, 2020. The Robert Koch Institute⁶ reports daily CoViD-19 cases and deaths for each of the 16 German states. This section reports on analyses of the 13 states reporting more than 2000 cases by the end of June 2020. Data between March 1 and June 25 are used, with exceptions that data after May 30 for Berlin and after June 18 for North Rhine-Westphalia are not used since localized outbreaks affected the case data for those periods.

A minimum of three constant growth periods are necessary to describe the observed rise and fall in daily cases in each of the states, with one transition (on day d_1) occurring before March 22 and another (d_2) near March 22. A third transition is forced on May 6, in order to estimate the growth following relaxation. Results from model fits to the data, showing the point estimates for the transition dates d_1 and d_2 and the growth rates are shown in Table 4. Figure 5 shows the cumulative distributions for cases and deaths for the first 45 days compared to the model predictions that use the fitted parameter values.

To estimate bias and standard deviations of the estimators, 200 simulated samples were produced using these point estimates, and fit keeping the transition dates fixed. The mean and standard deviations of the estimates are reported in Table 5. In separate studies, the standard deviations of transition date estimates were found to be typically 1 day. The estimated dates for the second transition has a mean of 22.6 days following March 1, and a standard deviation 2.4 days. The growth estimates, corrected for bias, are summarized along with their estimated standard deviations in Fig. 6.

Table 4. Point estimates for the four growth parameters from model fits to case data are shown for each state in Germany. The transition day estimates \hat{d}_1 and \hat{d}_2 were determined in the fit, and are shown as the day in March. Transition day d_3 was fixed to May 6, in order to estimate the growth parameter, δ_3 following relaxation of lock-down measures.

State	$\hat{\delta}_0$	\hat{d}_1	$\hat{\delta}_1$	\hat{d}_2	$\hat{\delta}_2$	$\hat{\delta}_3$
Baden-Warttemberg	0.288	12	0.105	24	-0.049	-0.060
Bavaria	0.256	14	0.160	23	-0.049	-0.041
Berlin	0.402	7	0.131	20	-0.038	-0.021
Brandenburg	0.345	10	0.102	26	-0.031	-0.086
Hamburg	0.410	9	0.122	20	-0.043	-0.061
Hesse	0.354	11	0.078	23	-0.031	-0.026
Lower Saxony	0.494	5	0.160	21	-0.039	0.002
North Rhine-Westphalia	0.274	5	0.134	22	-0.038	-0.029
Rhineland-Palatinate	0.483	9	0.075	23	-0.047	-0.028
Saarland	0.282	13	0.108	28	-0.073	-0.031
Saxony	0.426	10	0.108	23	-0.045	-0.033
Schleswig-Holstein	0.355	8	0.148	21	-0.041	-0.056
Thuringia	0.287	15	0.117	20	-0.017	-0.029

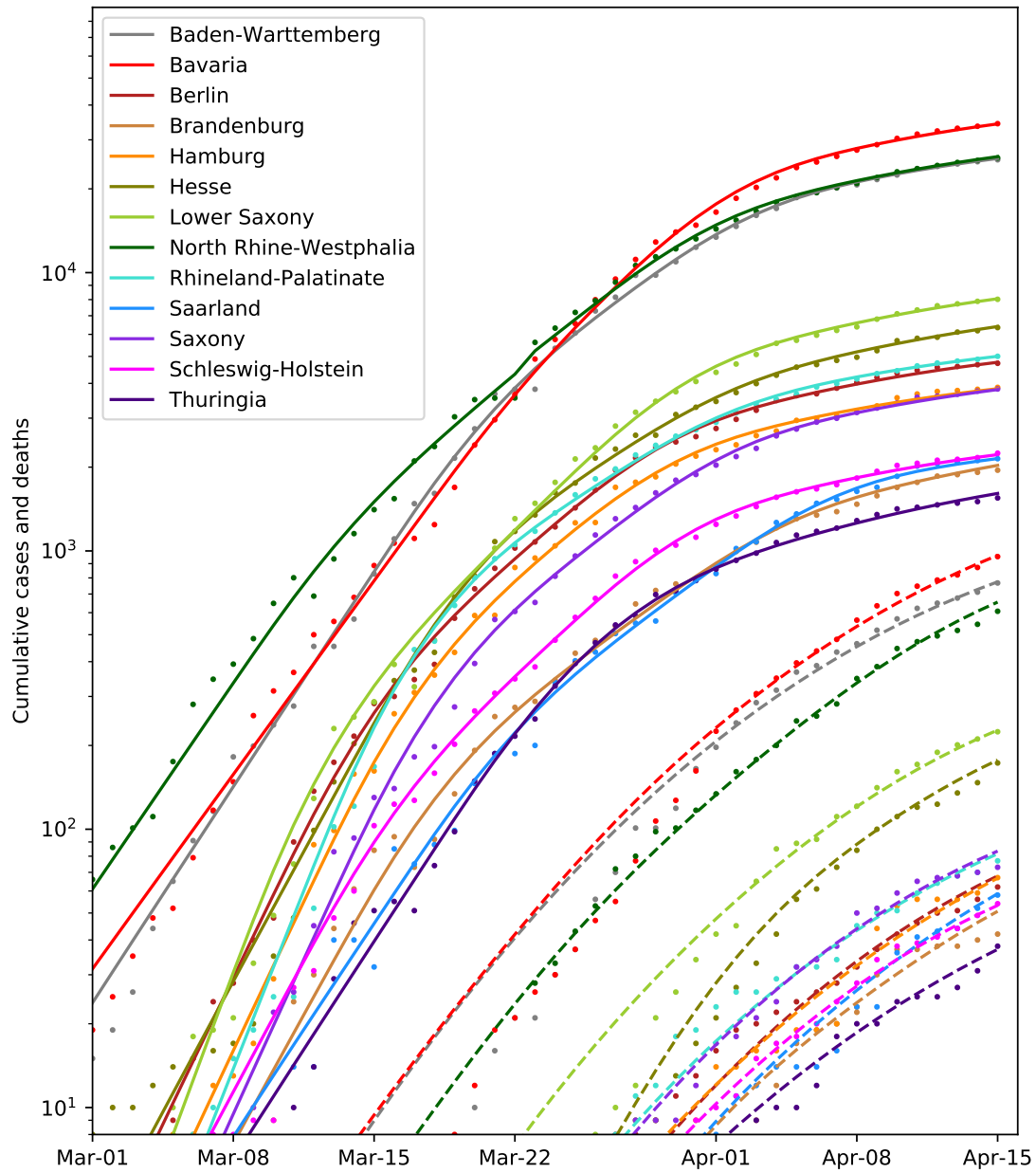


Figure 5. Cumulative case and death data (points) are shown in comparison to model predictions (lines) with the point estimates shown in Table 4 for the period March 1 - April 15, 2020. The dashed lines show the model predictions for the cumulative deaths during this period.

Table 5. To estimate bias and the standard deviations of estimators for the growth parameters, fits to 200 simulated samples using the point estimates from Table 4 were performed. The means and standard deviations of the estimates, shown here, do not indicate significant bias.

State	$\delta_0 (\mu, \sigma)$	$\delta_1 (\mu, \sigma)$	$\delta_2 (\mu, \sigma)$	$\delta_3 (\mu, \sigma)$
Baden-Wuerttemberg	0.283, 0.024	0.119, 0.007	-0.048, 0.002	-0.065, 0.009
Bavaria	0.238, 0.022	0.186, 0.011	-0.049, 0.002	-0.046, 0.010
Berlin	0.394, 0.036	0.150, 0.013	-0.038, 0.005	-0.036, 0.036
Brandenburg	0.342, 0.036	0.113, 0.019	-0.029, 0.007	-0.088, 0.027
Hamburg	0.401, 0.029	0.141, 0.016	-0.043, 0.005	-0.075, 0.031
Hesse	0.365, 0.039	0.096, 0.013	-0.031, 0.004	-0.029, 0.010
Lower Saxony	0.470, 0.019	0.175, 0.010	-0.038, 0.003	-0.001, 0.007
North Rhine-Westphalia	0.207, 0.046	0.156, 0.009	-0.037, 0.002	-0.033, 0.007
Rhineland-Palatinate	0.467, 0.023	0.092, 0.011	-0.046, 0.004	-0.037, 0.021
Saarland	0.264, 0.031	0.122, 0.015	-0.069, 0.009	-0.055, 0.043
Saxony	0.396, 0.031	0.132, 0.015	-0.045, 0.006	-0.041, 0.022
Schleswig-Holstein	0.332, 0.032	0.173, 0.024	-0.040, 0.007	-0.068, 0.032
Thuringia	0.295, 0.027	0.173, 0.056	-0.016, 0.006	-0.029, 0.013

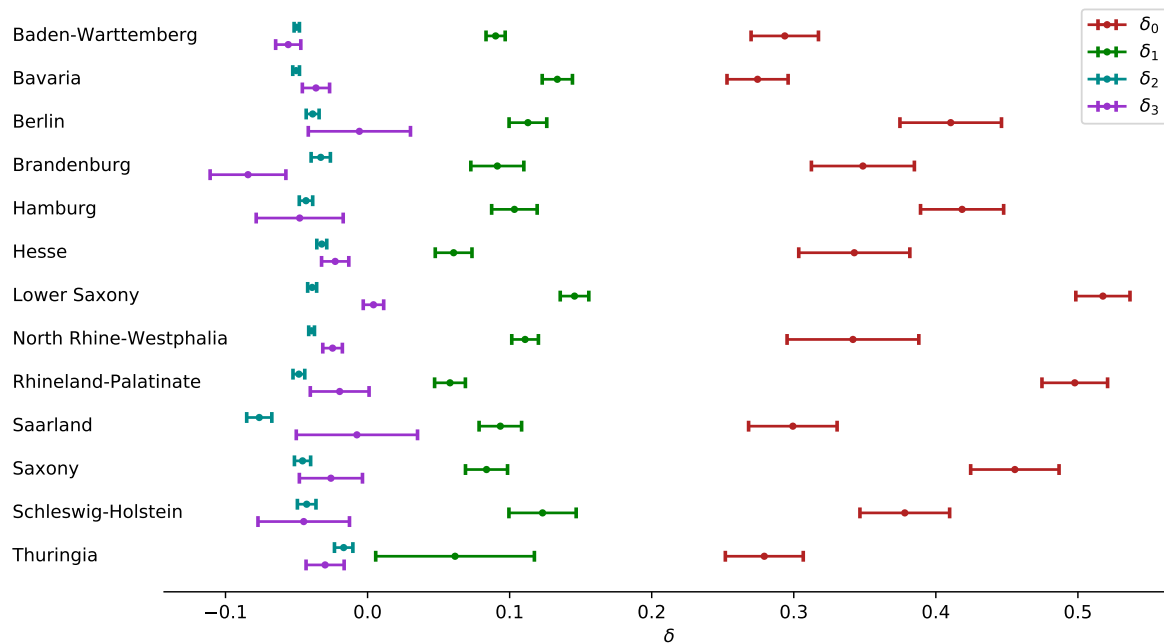


Figure 6. Summary of the growth rate estimates (corrected for bias) and their one standard deviation statistical uncertainties for the four periods for each state in Germany.

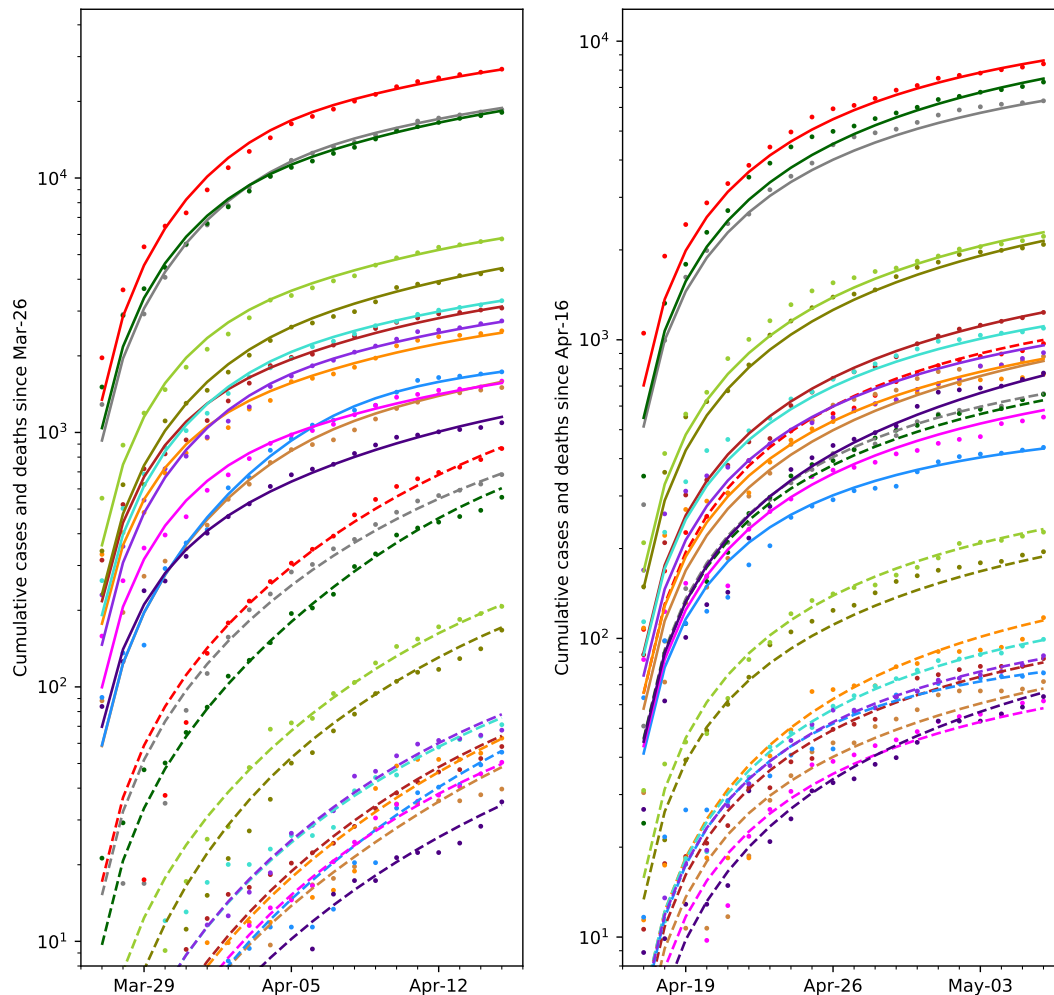


Figure 7. Cumulative case and death data (points) are shown in comparison to model predictions (lines) with the point estimates shown in Table 4 for the two periods (A-left) March 27 - April 15 and (B-right) April 17 - May 6. Lock-down measures were fixed across these two periods. The dashed lines show the model predictions for the cumulative deaths. The colors in the legend for Fig. 5 apply.

5.1 Test of statistical uncertainty of growth rate estimates

A test was performed for the statistical uncertainties assigned for growth rate estimates, by comparing estimates for the growth rates for two independent periods (A) March 27 - April 15 and (B) April 17 - May 6. Lock-down measures were fixed during this period, so growth rates would be expected to be nearly the same for the two periods. The cumulative cases and deaths for those periods are shown in Fig. 7

Model fits were performed using case data for those periods separately, by optimizing only the growth rate parameter, δ_2 , and the scale parameter C_0 (the initial size of the contagious population). The same approach was applied to 100 simulated samples using the point estimates shown in Table 4. The differences between the point estimates for the two periods, $\Delta = \hat{\delta}_{2A} - \hat{\delta}_{2B}$, for data and the simulated samples are summarized in Fig. 8. The hypothesis that the model correctly assigns a statistical uncertainty is tested using the χ^2 statistic, using the differences between the observed and expected Δ and the model estimates for σ_Δ . The statistic yields $\chi^2 = 18.1$ for 13 degrees of freedom, with the corresponding p-value= 0.15.

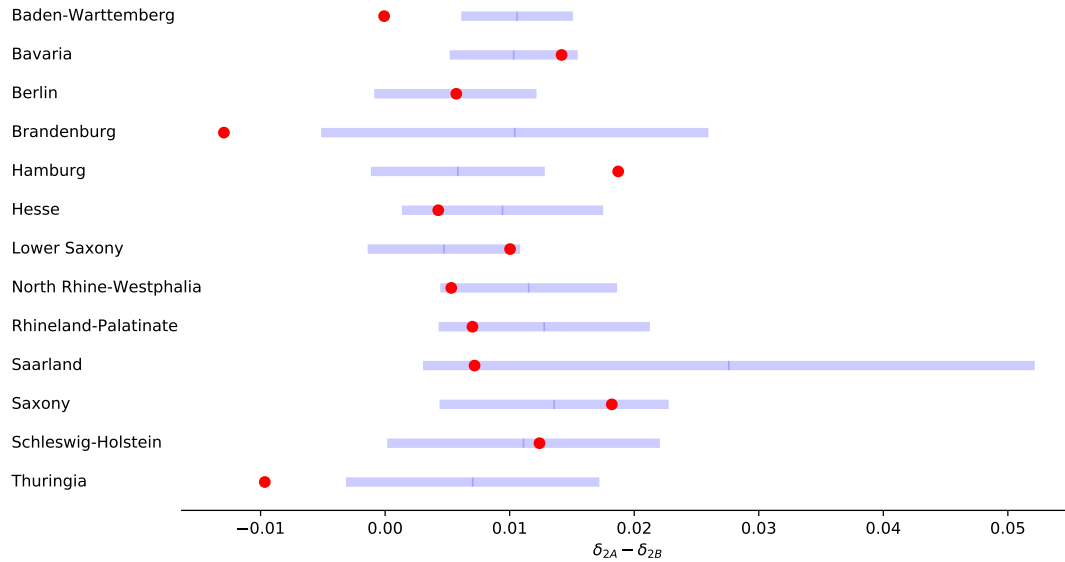


Figure 8. Difference in growth rate estimates for periods (A) and (B) during which lock-down measures were fixed. The red points show the data estimates. The blue bars show the mean and ± 1 standard deviations of the estimates from 100 simulated samples. The data estimates are consistent with being outcomes of the estimators defined by model fits: the goodness of fit test yields the p-value= 0.15.

5.2 Change in growth rate following relaxation of lock-down measures

As described above, a transition in transmission rates was forced on May 6, so that the estimated growth rate parameters before ($\hat{\delta}_2$) and after ($\hat{\delta}_3$) that date can be compared. The test of bias and statistical uncertainty shown in section 5.1 confirms the method to estimate the statistical significance of the observed difference in growth rate. After correcting the point estimates in Table 4 for biases deduced from fits to simulated samples as reported in Table 5, the weighted average difference of the point estimates for the 13 German states is $\hat{\delta}_3 - \hat{\delta}_2 = 0.0145 \pm 0.0035$, a small but statistically significant increase. Even with 50 days of data following relaxation, the growth rate estimates $\hat{\delta}_3$ have large uncertainty due to the diminishing numbers of cases.

5.3 Estimated size of epidemic

As discussed in section 3.4 the “uncorrected circulating contagious population” (or *UC*) is a useful comparative statistic for the size of the contagious population, with reduced systematic uncertainty. The *UC* history for each of the German states is shown in Fig. 9 relative to the state population. The relative sizes for different states were within a factor of about 5 throughout the period shown.

5.4 Estimated death delay time distribution

After estimating the transmission rates using the case data, the death delay distribution parameters are estimated in separate fits of the model to the cumulative death data. In these fits, the transmission rates are fixed to the point estimates in Table 4 and only three parameters are estimated; a scale factor (the fraction of the contagious who die), and the mean and standard deviation of the time between becoming contagious and death. The statistical uncertainty in these estimates are defined by the standard deviation of estimates from fits to 100 simulated samples. The results from each state are shown in Fig. 10. The data from the rapid rise in the death rate in the early stages of the epidemic carry the most information to estimate the standard deviation of the delay (σ_D). With larger values for σ_D , the rise in

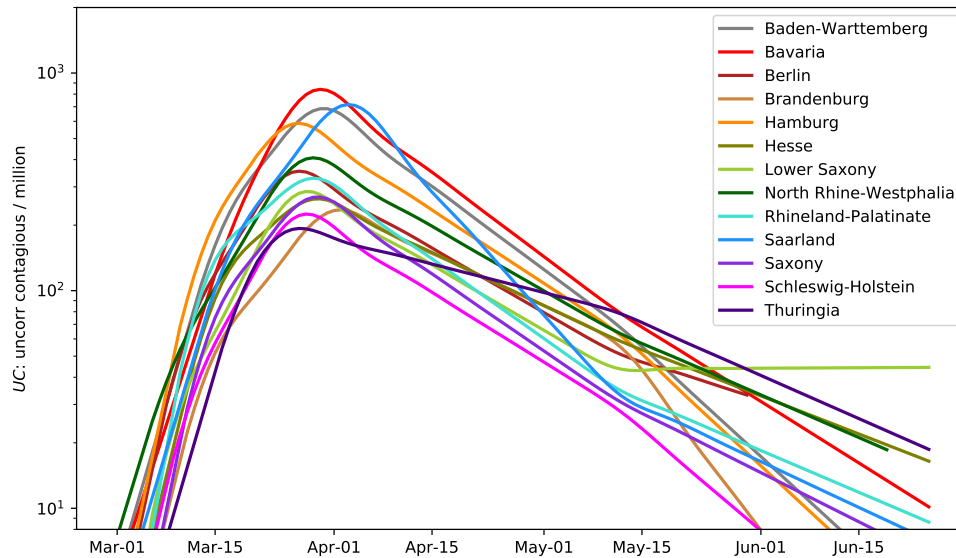


Figure 9. The uncorrected circulating contagious population history is shown for each state relative to the state population.

deaths is slower. The analysis is not sensitive to a long upper tail in the delay distribution, and the assumption that the distribution is normal may be incorrect.

The weighted average for the mean delay is 18.7 ± 0.3 days and for the standard deviation of the delay is 8.4 ± 0.4 days. Sources of systematic uncertainty on the mean delay arise from possible mis-modelling of other delays. Case and death report modelling have the latent delay in common, and since the fitted transition date \hat{d}_2 , is consistent with the expected transition (March 22), the systematic uncertainty from latent delay modelling could be assigned as the standard deviation of the observed transition dates, about 2.3 days. Including an additional 2 days for uncertainty in case reporting delays, and using the mean latent period in the model (5 days), the time distribution from infection to death is estimated to have a mean of 24 ± 3 days and a standard deviation of about 8 ± 1 days. The mean time from symptoms to death estimated with the pyPM model 2.3, 16.7 is consistent with the 95% credible interval [16.9|19.2] reported from an early study of 24 deaths in China.⁷

6 Summary and conclusions

The simple pyPM model, introduced in this paper, can be used to interpret public data in order to characterize the spread of CoViD-19 in different regions around the world. With relatively few parameters, the epidemic history can be conveniently summarized, with relatively long periods having constant transmission rates (reported with the daily growth parameters δ_i) and the size of the contagious population (reported with UC).

As governments relax social distancing rules and open borders, it will be important to compare the state of the disease and to detect changes in growth rates. As the situation develops, results from additional studies will be made available on the website www.pypm.ca.

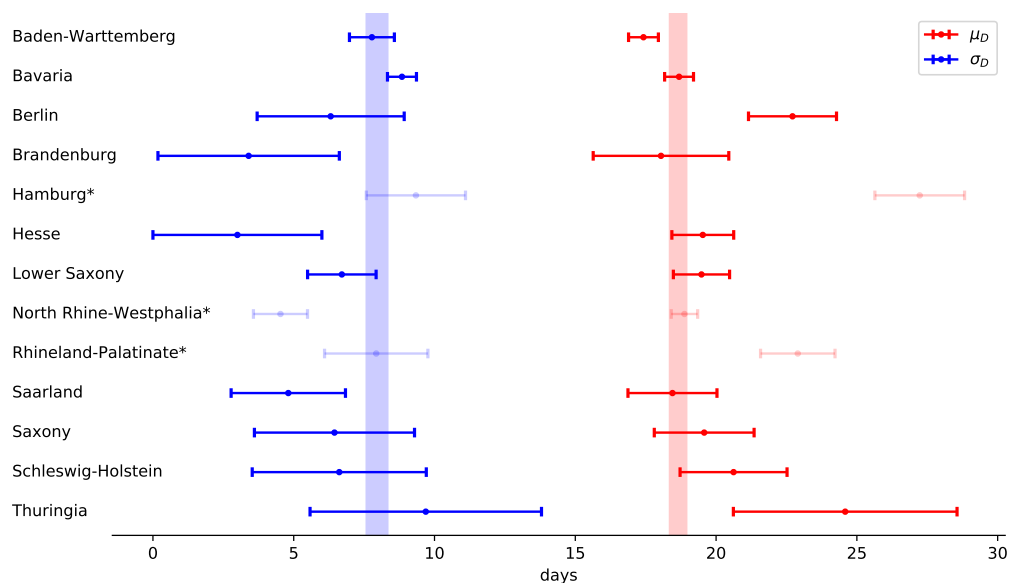


Figure 10. Estimates of the mean (μ_D) and standard deviation (σ_D) of the time between becoming contagious and death. The states indicated with '*' and shaded out have one of their estimates more than 3σ from the full weighted average and are not used in the reported weighted averages. The vertical bars indicate the weighted averages and 68% CL statistical uncertainty.

References

1. pyPM: python Population Modeller ; URL <https://www.pypm.ca>.
2. Li J, Blakeley D and Smith RJ. The Failure of R_0 . *Computational and Mathematical Methods in Medicine* 2011; DOI: 10.1155/2011/527610.
3. Wallinga J and Lipsitch M. How generation intervals shape the relationship between growth rates and reproductive numbers. *Proc Biol Sci* 2007;274(1609):599-604 2007; DOI:10.1098/rspb.2006.3754.
4. PHAC. Public Health Agency Canada Modelling Group weekly report, June 11 2020; .
5. BCCDC. British Columbia COVID-19 Daily Situation Report, June 18 2020; .
6. The Robert Koch Institute ; URL <https://www.rki.de>.
7. Verity R, Okell LC, Dorigatti I et al. Estimates of the severity of coronavirus disease 2019: a model-based analysis. *The Lancet Infectious Diseases* 2020; 20(6): 669 – 677. DOI:[https://doi.org/10.1016/S1473-3099\(20\)30243-7](https://doi.org/10.1016/S1473-3099(20)30243-7). URL <http://www.sciencedirect.com/science/article/pii/S1473309920302437>.